1985ApJ...291..865A

THE ASTROPHYSICAL JOURNAL, 291:865–878, 1985 April 15
© 1985. The American Astronomical Society. All rights reserved. Printed in U.S.A.

ROCKET SPECTROGRAM OF A SOLAR FLARE IN THE 10–100 Å REGION

L. W. ACTON, M. E. BRUNER, AND W. A. BROWN
Lockheed Palo Alto Research Laboratory
B. C. FAWCETT
Rutherford-Appleton Laboratories
W. SCHWEIZER
Institut fur Physikalische Messtechnik
AND
R. J. SPEER
Imperial College of Science and Technology
Received 1984 June 25; accepted 1984 November 1

ABSTRACT

The soft (10–100 Å) X-ray spectrum of an M-class solar flare was observed with a high-resolution (0.02 Å) rocket-borne spectrograph on 1982 July 13. The spectrum samples an area of ~ 600 arcsec^2 on the Sun, centered on or near the brightest X-ray feature of the flare. Several hundred emission lines characteristic of temperatures from about 0.5 to 7×10^6 K have been photographically recorded. All but three of the stronger lines have been identified. It is argued that previous identification of the line at 17.62 Å as iron Lyα is incorrect. Spectral lines from nickel, iron, chromium, calcium, sulphur, silicon, aluminium, magnesium, neon, oxygen, nitrogen, and carbon are tabulated and discussed with extensive references to earlier work. Absolute line intensities are given and the calibration of the telescope-spectrograph is discussed.

Subject headings: line identifications — Sun: flares — Sun: spectra — Sun: X-rays

I. INTRODUCTION

A 5 m grazing-incidence spectrograph with a 632 lines mm^{-1} grating was launched on a rocket on 1982 July 13 and acquired a solar flare spectrogram on film extending from 11 to 97 Å. Unique data were retrieved, first by reason of the higher spectral resolution achieved over much of the spectrogram and second because parts of the spectral region covered have not previously been recorded during a solar flare with similar instrumentation. The spectrograms longward of 23 Å therefore revealed many new solar flare lines while the higher spectral resolving power aided line identification.

Existing spectral data covering this wavelength region are of three kinds: First are the X-ray crystal spectrometer records both of flares (McKenzie and Landecker 1982*a*; McKenzie *et al.* 1980; Phillips *et al.* 1982) and of the active Sun (Hutcheon, Pye, and Evans 1976; Parkinson 1975; Pye, Evans, and Hutcheon 1977). Second are grazing-incidence spectrograms (Behring, Cohen, and Feldman 1972; Freeman and Jones 1970). In the third category are the grazing-incidence spectrometer data of Manson (1972) and Malinovsky and Heroux (1973). The crystal spectrometer records still provide the most detailed and precise observations below 23 Å. One of the best previous grazing-incidence spectrograms is that of Behring, Cohen, and Feldman (1972), who flew a 3 m instrument with a 1200 lines mm^{-1} grating and obtained active Sun spectra above 60 Å with resolution comparable to ours. Our new spectra add to this data base by showing new flare lines between 60 and 97 Å. The other high-quality grazing-incidence record was obtained by Freeman and Jones (1970) who flew a 0.5 m instrument, SL801, with a 1200 lines mm^{-1} grating and presented spectra of the Sun between 15 and 96 Å under less active coronal conditions and with significantly lower resolution than the present spectra. Finally, our spectra duplicate more solar lines previously recorded by crystal spectrometers than ever before. This is of some interest not only because of the comparison but also because, for certain diagnostic purposes, lines below 23 Å may need recording on the same instrument as those at longer wavelengths.

II. OBSERVATIONS

a) Instrument

Instrumentation for the experiment included a high-resolution grazing-incidence X-ray spectrograph and collecting mirror, an ultraviolet filtergraph, and an Hα imaging system. A complete discussion of the system has been given elsewhere (Bruner *et al.* 1980; Brown *et al.* 1979). Only a brief description of the X-ray spectrograph as configured for the 1982 flight will be given here.

The spectrograph optics are illustrated in Figure 1. Parallel light from a distant source strikes the collecting mirror at a glancing angle of 3°. The mirror, an extreme off-axis parabola, concentrates radiation traveling parallel to the optic axis onto an entrance slit located at the focus. The entrance slit, actually three slits in series along the chief ray, serves both to limit the field of view and to strongly attenuate visible light through diffraction effects (Schmidtke 1970; Schweizer and Schmidtke 1971). There is no filter.

Radiation passing through the entrance slit assembly strikes a concave diffraction grating at a glancing angle of 2°. The dispersed spectrum is recorded on X-ray–sensitive roll film (Kodak type 101-07) which is clamped to curved metal rails defining the Rowland cylinder. Exposure times are controlled by a mechanical shutter (not shown) located just in front of the film transport mechanism.

The spectrograph was designed and built at Lockheed using

© American Astronomical Society • Provided by the NASA Astrophysics Data System

1985ApJ...291..865A

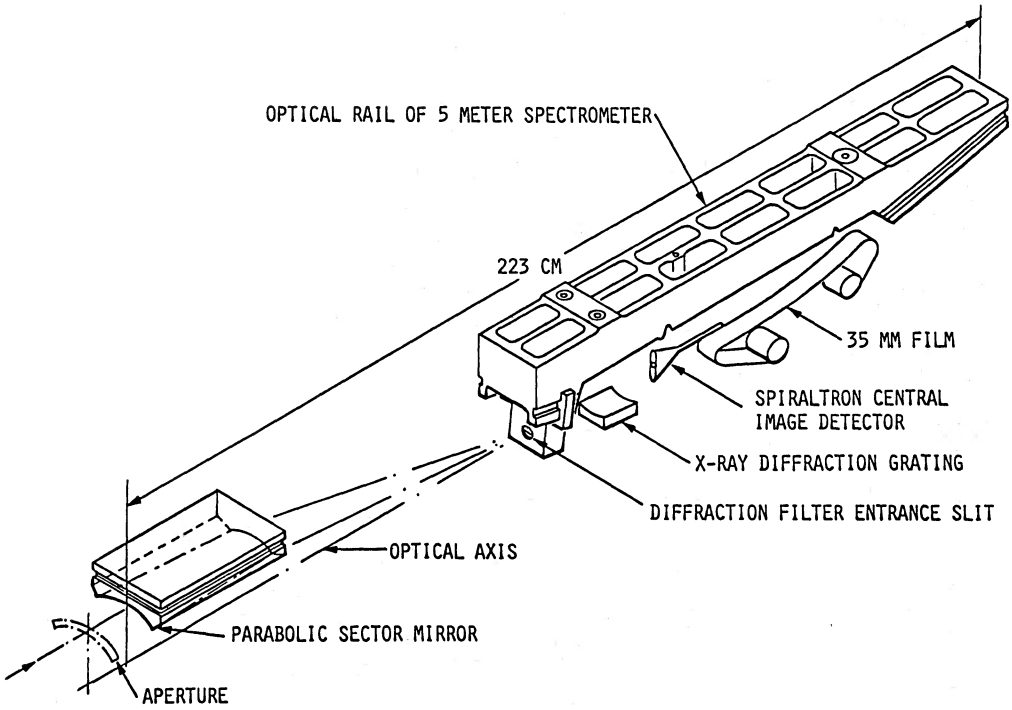

FIG. 1.—X-ray spectrograph telescope. Parallel light from a distant source strikes the collecting mirror at a glancing angle of 3°, is concentrated on the entrance slit assembly, and strikes a concave diffraction grating at a glancing angle of 2°0. The dispersed spectrum is recorded on X-ray–sensitive roll film (Kodak type 101-07), which is clamped to curved metal rails defining the Rowland cylinder. The radius of the Rowland circle is precisely 50 mm greater than that of the optical rail.

concepts from the 5 m GML5M laboratory instrument designed by R. J. Speer and D. Turner at Imperial College, London. Focus and alignment within the spectrograph are mechanically determined by an accurately machined aluminum optical bench to which the optical components are mounted. The curved rails of the optical bench form a cylinder of 245 cm radius, exactly 50 mm shorter than that of the Rowland cylinder. Thus the Rowland cylinder is defined to be exactly 50 mm above the rails of the optical bench, and optical components are placed on it through the use of mechanical metrology and lapping techniques. The resultant instrument is extremely rugged and resistant to vibration-induced misalignment, yet can be easily reconfigured to accommodate different gratings, detector systems, and wavelength ranges.

A photoelectric X-ray detector, sensitive to a broad band of wavelengths between about 8–15 and 44–60 Å, serves as an X-ray radiometer. It is used to indicate the relative intensities of X-ray–emitting regions and to locate the brightest region for study with the spectrograph.

Not shown in the figure are an Hα optical system and an ultraviolet filtergraph. The Hα system provided a video image at 6563 Å for use in initial selection of the region to be observed and for attitude information. The ultraviolet filtergraph (Bonnet *et al.* 1980) recorded very high resolution images of the solar disk in the H Lα line (1215 Å), lines and continuum in the vicinity of 1650 Å, and the UV continuum at 2200 Å.

b) Rocket Flight

The experiment was launched at 1630 UT on 1982 July 13, using a Nike-boosted Black Brant V vehicle. The payload reached an altitude of 303 km and provided 393 s of observing time under solar fine-pointing control. Prior to launch, our objective had been to record the X-ray spectrum of the corona over NOAA active region 3804. At T − 5 minutes, we were alerted by the observer at Big Bear Solar Observatory to the onset of a flare in our secondary target region, NOAA 3806, and this became the subject of the experiment.

Following launch and acquisition of the Sun by the SPARCS pointing system, we used the on-board Hα television image to identify the location of the flare and adjust the attitude-control system to place the flare near the optic axis of the spectrograph. Final pointing selection was made with a two-phase raster search pattern, in which the X-ray radiometer was used to map the X-ray brightness distribution.

Two exposures were made; one of 54 s beginning at 1633:50 UT and the other of 145 s beginning at 1635:35 UT. These times bracket the time of the soft X-ray maximum as defined by the *GOES* satellite observations. The film transport was commanded to advance between exposures. Unfortunately, the transport mechanism failed to unclamp the film on this one occasion, with the result that the film advanced only 0.5 mm, rather than the normal 25–30 cm. This was enough to separate the two spectra so that comparative analysis was still possible. Tension placed on the film by the unsuccessful transport attempt caused it to bow slightly into the slot between the camera rails, and the lines from the second exposure show a noticeable curvature toward the grating. The Kodak type 101-07 film was processed in D-19 developer according to the manufacturer's recommendations.

III. DATA ANALYSIS

a) Field of View

The results presented here are from the second, longer, exposure. These data refer to an interval about 2 minutes after the

© American Astronomical Society • Provided by the NASA Astrophysics Data System

1985ApJ...291..865A

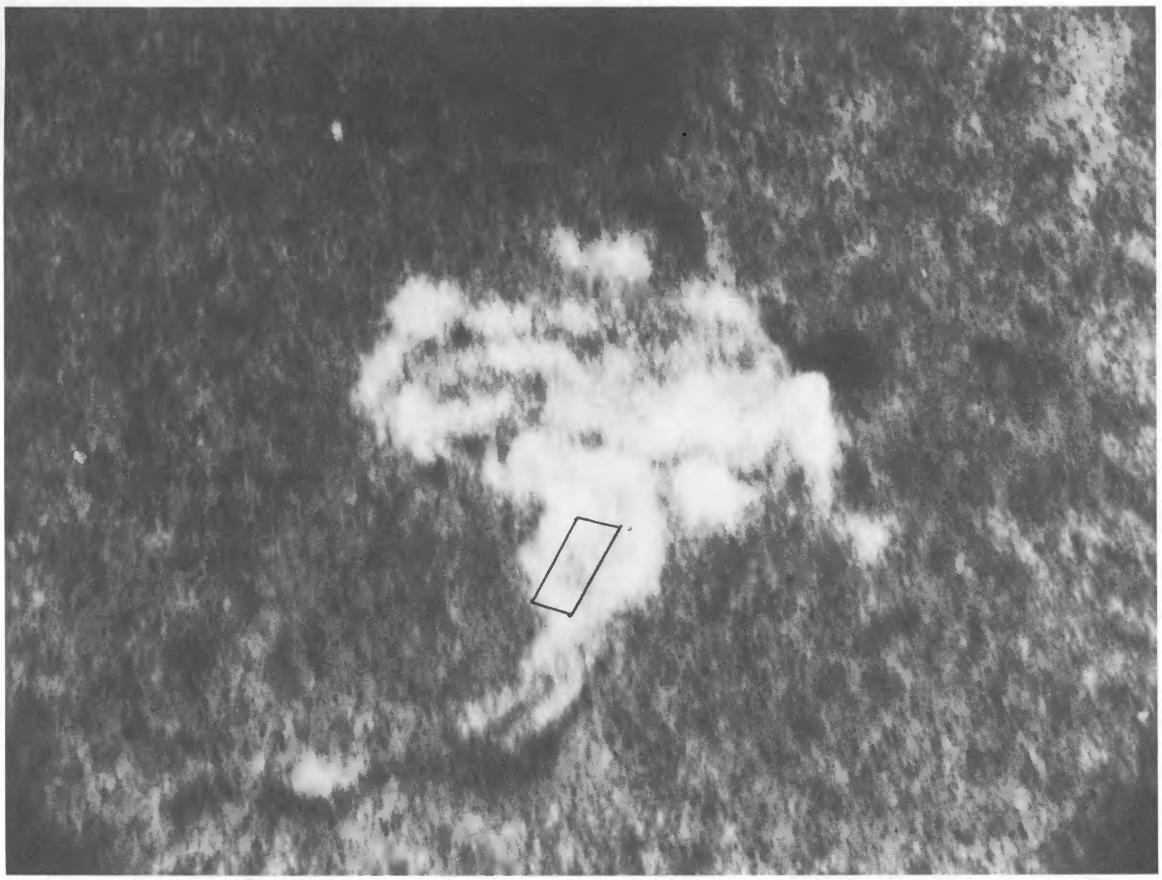

FIG. 2.—Hα image at 1632 UT (courtesy Caltech). The parallelogram outlines the regions sampled by the spectrograph during the 154 s exposure beginning at 1635:33 UT. North is at top and the long dimension of the parallelogram is 30″.

soft X-ray maximum of an M1 flare (NOAA 1–8 Å X-ray classification). The location and orientation of the instrument field of view on the flare is illustrated in Figure 2 and discussed in Acton *et al.* (1983). The recorded spectrum averaged over a solid angle of approximately 625 arcsec^2, centered on or near the brightest source of X-rays.

Any given element along the astigmatic line image is the result of energy collected from a rectangular field on the Sun of about 1.2 × 28 arcsec. The angular orientation of the rectangle on the solar disk is a function of the position of the image element along the astigmatic line, so that an average over the entire length of the image represents an hourglass-shaped figure on the Sun (Brown *et al.* 1979). While this figure encompasses an area larger than that of the projected slit, not all parts of the figure contribute equally, so that the equivalent solid angle of the instrument is still that of the nominal 1.2 × 28 arcsec field. The effects of the aberrations, together with those of commanded attitude changes during the 145 s exposure, account for the comparatively large effective size of the spectrograph field of view for this spectrogram.

b) Densitometry of the Spectrogram

Figure 3 is a negative print of the spectrogram. Despite the film distortion caused by the malfunction of the film transport, the 0.02 Å design value for spectral resolution appears to have been achieved or surpassed over most of the spectrogram. Some of the atomic ions contributing to the spectrum are identified. A strong second-order spectrum falling between 25 and 50 Å is evident. The distracting effects of scattered light and double exposure, although mostly cosmetic, have made the reduction of these data difficult.

The photographic prints of Figure 3 were prepared from a high-contrast fine-grain positive transparency (Kodak Technical Pan TP-2415) contact printed from the original flight film. In an attempt to enhance the many weak spectral features present, the flight film was put through autoradiographic processing (Askins, Craven, and O'Dell 1979; Askins and O'Dell 1980). This experiment appeared successful, in that many lines of weak-to-intermediate strength were more evident on the radiograms, but many of the faintest features appeared to be lost in grain noise. This impression was borne out by a poorer signal-to-noise ratio in microdensitometer tracings of the radiogram as compared to the original flight film. Therefore the autoradiographic microdensitometer tracings were not used in the data analysis. Densitometry was carried out at Lockheed on a computer-controlled PDS microdensitometer, on which densities are recorded relative to a Kodak neutral-density step wedge. Scanning of the spectrum was done along 75 strips, each 125 μm wide, so that numerical correction of the image curvature could be done as part of the analysis.

c) Intensity Calibration

The response of the X-ray spectrograph–telescope to solar X-ray–line emission was established by comparison to laboratory sources. This was done in two stages so that the response of the complete instrument could be compared to the combination of the component efficiencies. The following expression relates the intensity of a spectral line to instrumental

© American Astronomical Society • Provided by the NASA Astrophysics Data System

1985ApJ...291..865A

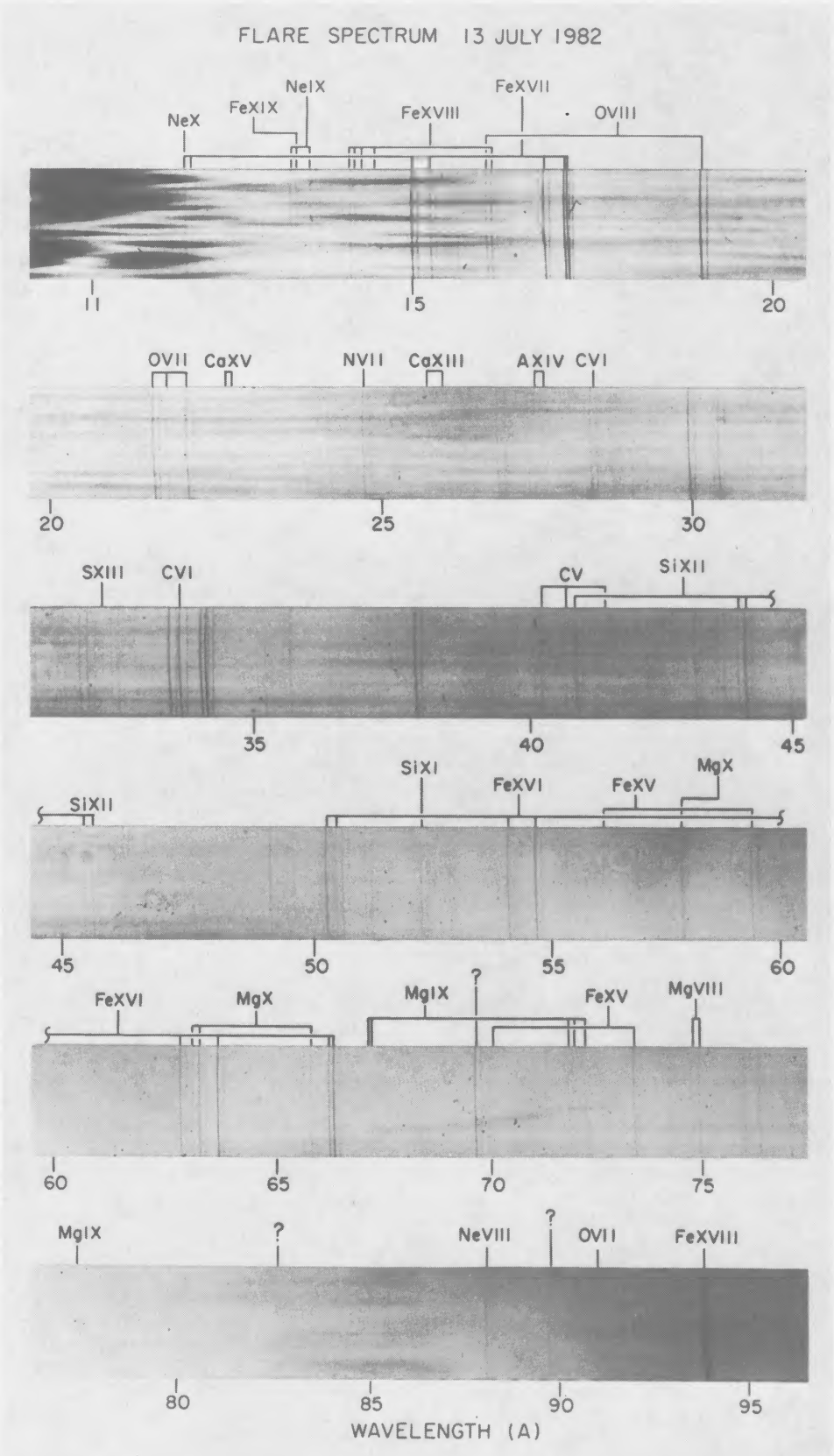

FIG. 3.—Negative print of the solar X-ray spectrogram of 1982 July 13. Some of the atomic ions contributing to the spectrum are identified. A strong second-order spectrum falling between 25 and 50 Å is evident. A film transport defect caused two exposures of 45 and 154 s duration to nearly coincide. Over 400 lines in the darker spectrum have been tabulated.

© American Astronomical Society • Provided by the NASA Astrophysics Data System

1985ApJ...291..865A

properties and density measurements from the flight film:

$$\text{Intensity} = U_\lambda\, dw \text{ photons cm}^{-2}\text{ s}^{-1}\text{ arcsec}^{-2}\,. \quad (1)$$

Here the peak density (d) and FWHM width (w) are obtained from manipulating the densitometer scan data so that curved lines are straightened and line widths are measured in units of the 24 μm densitometer step. The function U_λ includes all the wavelength-dependent sensitivity information. We write

$$U_\lambda = \frac{0.0024 L_\lambda (E/d)_\lambda}{AT\,\Omega\, Em_\lambda\, Eg_\lambda}\,, \quad (2)$$

where L_λ = line length from full mirror width, $(E/d)_\lambda$ = exposure/density for this film (where exposure units are photons cm^{-2}), A = effective mirror area for full mirror width, t = exposure time (145 s for the exposure discussed here), Ω = 33 arcsec^2 (the nominal field of view), Em_λ = efficiency of the paraboloidal telescope mirror, Eg_λ = efficiency of the concave spectrograph grating.

Line length and mirror area are not independent, but the ratio used here is independent of mirror width. That is, the mirror area is proportional to the width of the mirror and the astigmatic spectral line length is proportional to the same quantity. The ratio reflects the greater line length of the long wavelength lines. For the full 10 cm mirror width, the line length at 13 Å is 4 cm, while at 100 Å it is 6.9 cm. The effective mirror area of 5 cm^2 is half the full projected area because the triple diffraction slit used here vignettes the mirror.

The reflectivity of the gold-coated paraboloidal collecting mirror was measured at 8.34, 13.3, and 44.7 Å. The measurements are higher than the predictions of Ershov, Brytov, and Lukirskii (1967), but good agreement was found between the Lockheed measurements and those made at Imperial College. The flight grating, NPL 172, was recoated in April 1982 by Astron, Ltd., and measured both at Lockheed and at Imperial College. Measurements were made at three positions on the grating, as this influences the angle of incidence. First-order efficiency was measured at the Kα wavelengths of Al, O, C, B, and Be plus the Lyα line of Cu.

The response of Eastman Kodak 101 emulsions was tested at normal incidence and at 12° grazing incidence. This film, when exposed to soft X-rays at grazing incidence, exhibits a saturation effect at densities above 0.2. At the low densities found in our data, however, only the effect of geometric projection was evident. The film response was compared to that of a proportional counter purchased from the J. E. Manson Company. The counter was filled with 320 torr of P-10 methane/argon mixture and the transmission of its window was measured to determine its efficiency. Table 1 summarizes instrument performance parameters and the instrument sensitivity function, U_λ, found by combining the effects discussed above. The experiment error in each individual measurement is judged to be less than 20%.

TABLE 1

INSTRUMENT SENSITIVITY

Wavelength	E/d[a]	Em	Eg	$\log_{10} U_\lambda$ Computed	$\log_{10} U_\lambda$ Lin. Fit[b]
8.34	3.1(8)	0.20	0.05	4.061	3.827
13.36	3.5(8)	0.46	0.08	3.582	3.566
23.66	*3.3(8)	*0.47	0.15	3.325	3.378
43.44	2.9(8)	0.65	0.13	3.261	3.266
67.38	3.2(8)	*0.75	0.14	3.271	3.219
113.74	2.1(8)	*0.96	0.106	3.115	3.184

NOTE.—Starred values were obtained by extrapolation or interpolation.
[a] Exposure in units of photons cm^{-2}.
[b] Linear fit to the computed values.

To simplify the task of assigning intensities to the lines, values in this table were approximated with the following function (λ = wavelength in Å), tabulated in the last column of Table 1:

$$\log_{10} U_\lambda = 5.7916/\lambda + 3.133 \quad (3)$$

Second-order line intensities were usable for many lines. Measurements of grating efficiency in second order were used to construct Table 2 of the intensity function. Since many lines were seen in both first and second order, a comparison was made to develop confidence in our assignments of intensities to lines for which only the second order is present or usable. Comparison of first- and second-order intensities showed half within 50%. The strongest lines agreed within 10%. The computed function $\log_{10} U_\lambda$ was plotted and graphically interpolated in assigning intensity values to the second-order lines.

The presence of a thin carbon overcoat on the reflective surfaces may not be ruled out since the payload was pumped with systems that are not free of hydrocarbon contamination, although an attempt was made to hold this to a minimum. The flight data, unlike the laboratory calibration exercises, contained spectral lines on both sides of and in close proximity to the carbon absorption edge at 43.8 Å. Examination of line intensity ratios of Si XI, Si XII, and Fe XVI gave ambiguous results concerning the presence or absence of C absorption. This is attributed to the inadequacy of published line-intensity predictions. Therefore, the line intensities presented in Table 3 assume no sensitivity jump at the C K-edge and are derived from a smooth curve drawn through the sensitivity values of Table 1. It must be noted that we believe a K-edge discontinuity as large as a factor of 2 would be allowed by our present understanding of the data, so that line strengths just shortward of the C K-edge should be viewed with caution.

The reported intensities are based on averages of the measured densities along the full length of the curvature-corrected second exposure lines. Intensities are given for first- and second-order images except where blending was a problem. In

TABLE 2

SECOND-ORDER SENSITIVITY FUNCTION

Wavelength (Å) First Order	Wavelength (Å) Second Order	Em	Eg	E/d	L (cm)	$\log_{10} U_\lambda$
8.34	16.7	0.2	0.04	3.1(8)	4.2	4.213
13.3	26.6	0.46	0.065	3.5(8)	4.6	3.733
23.3	46.6	0.47	0.06	3.3(8)	5.3	3.794

© American Astronomical Society • Provided by the NASA Astrophysics Data System

1985ApJ...291..865A

some cases first-order intensities have been used to correct second-order blends with first-order images. Intensities are not given for hopelessly blended lines, nor for lines with solar intensity below 10 photons cm^{-2} s^{-1} $arcsec^{-2}$. The lowest densities used ranged from 0.0004 to 0.0015, while no density exceeded 0.1.

IV. RESULTS

a) Line Identifications

The approximately 430 spectral features measured on this spectrogram are presented in Table 3. Wavelengths have been determined in most cases from the tracings. In general there is good agreement with published values but we do not claim an accuracy better than ± 0.02 Å because of our film-distortion problem. The curvature of the long (second) exposure lines has helped to exclude spurious entries that might result from the double exposure. Line identification has been based on wavelength agreement and multiplet predictions.

The spectra can be conveniently described by taking together solar-abundant elements which are nearby in the periodic table.

b) Iron, Nickel, and Chromium Spectra

The iron spectrum is well represented in ionization stages from Fe XIV to Fe XIX, with Fe XX and Fe XXI also present. Fe XIII and lower stages have their dominant lines outside the 11–97 Å spectral region. Predictably, the solar flare spectra of Fe XVII are intense along with many lines of Fe XVIII. Published data on the classification of these ions is firm (Feldman *et al.* 1973). This is not the case for Fe XIX, where only the more reliable identifications are listed in the table of identifications. Although better-quality solar-flare spectra of Fe XVII to Fe XXI exist on crystal spectrometer records, these spectra of Fe XIV, Fe XV, and Fe XVI are the most comprehensive solar spectrograms of these ions to date. The Fe XVI spectra are well represented, with more than one member of the series. In Fe XV not only are the singlets intense, excited by routes from the ground, but also the triplets appear. Although the triplets are weaker than in dense plasmas, their appearance at considerable intensity points to their origin at solar-flare densities rather than at coronal densities, where population of levels directly from the ground state is preferred. Nickel spectra follow the same rules but are rather weak due to the element's lower abundance. A few weak chromium lines are visible.

The line at 17.62 Å has been identified as the Lyα transition of neutral or low-ionization iron by McKenzie *et al.* (1980) and Phillips *et al.* (1982). McKenzie and Landecker (1982*a*) question this identification on wavelength (they measure 17.626 Å) and intensity grounds. Our best wavelength for this line is 17.618 Å (first order) and 17.621 Å (second order). Phillips *et al.* (1982) quote 17.622 Å. These are all well determined wavelengths, probably within 0.01 Å. Bearden (1967) gives 17.59 ± 0.02 Å for the Fe Lyα line. Thus the Lα identification is marginal based on wavelength agreement. Furthermore, the laboratory Lyα line is broad. Two-crystal spectrometer measurements at New Mexico State University (A. Burr, private communication) yield a resolved width of approximately 3 eV (0.075 Å). The solar line is unresolved at a spectrograph resolution of 0.02 Å. In the case of Fe Kα, the solar line is as wide as the laboratory line (Parmar *et al.* 1984) and, although the reason for the broadening is not well understood, it is reasonable to expect that the solar Fe Lyα would also reflect the excess width of the laboratory line. Therefore, we reject the Lyα identification on both wavelength and line-width grounds. The unclassified Fe line listed by Cohen and Feldman (1970) at 17.622 Å from low-inductance vacuum-spark measurements is probably the same transition as the solar line.

c) Calcium and Argon

The calcium solar flare lines recently identified by McKenzie and Landecker (1982*a*) in SOLEX solar-flare crystal spectra are observed, along with new identifications of Ca XI to Ca XV resonance lines. We record only the density-insensitive component $2p^2\ {}^3P_0$–$2p3d^3D_1$ of the pair of Ca XV lines listed by McKenzie and Landecker (1982*a*) at 22.733 and 22.778 Å. The electron density, 2×10^{10} cm^{-3}, derived from the helium-like O VII lines is consistent with our nondetection of the $2p^2\ {}^3P_2$–$2p3d^3D_3$ transition. Because of the wavelength standard provided by the nearby O VII, lines we believe our wavelength of 22.712 Å for the $2p^2\ {}^3P_0$–$2p3d^3D_1$ transition to be significantly discrepant to the McKenzie and Landecker wavelengths.

Surprisingly, even the strongest expected argon lines (Ar IX) could not be found.

d) Magnesium, Aluminum, Silicon, and Sulfur

Again these spectrograms present perhaps the most extensive solar observations in this spectral region of the $n = 2$–3 transitions for these elements, along with some involving higher principal quantum number. The silicon spectrum is the best developed with Si XII, XI, X, IX, and VIII represented and $n = 2$–4 transitions also present. Next in order of dominance is the magnesium spectrum with Mg X, IX, and VIII. The most original contributions in the entire spectrum are perhaps the new solar identifications in sulfur where S XIV, XIII, XII, XI, and X lines are found. A few lines of Al XI, X, and VIII are visible. In each of these elements the Li-like and the Be-like spectra tend to be the most prominent.

e) Light Elements: Carbon, Nitrogen, Oxygen, and Neon

The H-like and He-like lines of these elements are present. The He-like ^1S–^3P intercombination and ^1S–^3S forbidden lines are present in C, O, and Ne at useful intensities for diagnostic purposes, but the Li-like satellites to the He-like ^1S–^1P resonance line are too weak for the type of diagnostics possible with crystal solar-flare spectrograms.

f) Strong Unidentified Lines

Of the prominent lines recorded on this experiment only four, at 17.62, 69.65, 82.76, and 89.76 Å, remain unidentified. The 69.65 Å solar line has been recorded by several experiments and has been identified as an Fe XIV or a Si VIII line or both. However, the wavelengths do not agree well and, in our spectrum, it is too intense for either candidate. Furthermore, our data and those published by Widing and Sandlin (1968) show this line to be strongly enhanced by solar activity. It is to be hoped that, when identified, these lines will turn out to be diagnostically useful for coronal studies.

V. CONCLUSION

The solar spectrum between 23 Å and 130 Å has received comparatively little attention, and observations are not of the quality possible with state-of-the-art technology. The data pre-

© American Astronomical Society • Provided by the NASA Astrophysics Data System

1985ApJ...291..865A

TABLE 3

PHOTOGRAPHIC SOLAR FLARE SPECTRUM, 9–93 Å

Observed Wavelength Å	Intensity units*	Order	Ion	Previous Solar Wavelength Å	Selected Previous Measurement Å	Multiplet	J-J'	Transition Array	Solar References	Other References
11.53	b	1	Fe XVIII	11.525	11.526	^{2}P-(^{3}P)^{2}D	3/2-3/2 , 5/2	2p^5-2p^{4}4d	22	1
	b		Fe XVIII	11.545	11.551	^{2}P-(^{3}P)^{2}P	1/2-3/2	2p^5-2p^{4}4d	22	4,14
	b		Ne IX		11.5466	1S-^{1}P	0-1	1s^2-1s3p		6
12.12	b	1	Fe XVII	12.122	12.123	1S-^{1}P	0-1	2p^6-2p^{5}4d	22	14
	b		Ne X	12.132	12.1339	^{2}S-^{2}P	1/2-1/2 , 3/2	1s-2p	22	6
12.25		1	Fe XVII	12.263	12.263	^{1}S-^{3}D	0-1	2p^6-2p^{5}4d	22	14
12.82	b	1	Ni XIX	12.812	12.812	^{1}S-^{3}P	0-1	2p^6-2p^{5}3d	22	13
	b		Fe XX	12.812	12.80	^{4}S-(^{3}P)^{4}P	3/2-1/2	2p^3-2p^{2}3d	22	3
	b		Fe XX	12.827	12.82	^{4}S-(^{3}P)^{4}P	3/2-3/2	2p^3-2p^{2}3d	22	3
	b		Fe XX	12.846	12.84	^{4}S-(^{3}P)^{4}P	3/2-5/2	2p^3-2p^{2}3d	22	3
13.45	318	1	Ne IX	13.446	13.4471	^{1}S-^{1}P	0-1	1s^2-1s2p	22,23	7
13.51	274 b	1	Fe XIX	13.504	13.506	^{3}P-(^{2}D)^{3}P	2-2	2p^4-2p^{3}3d	22,23	2,20,27
	b		Fe XIX	13.520	13.521	^{3}P-(^{2}D)^{3}D	2-3	2p^4-2p^{3}3d	22	2,27
13.55	86 b	1	Ne IX	13.551	13.5529	^{1}S-^{3}P	0-1	1s^2-1s2p	22	7
13.70	264	1	Ne IX	13.698	13.6987	^{1}S-^{3}S	0-1	1s^2-1s2s	22	7
13.78	180 b	1	Ni XIX	13.777	13.779	^{1}S-^{1}P	0-1	2p^6-2p^{5}3s	22,23	14
			Fe XIX	13.796	13.796	^{3}P-(^{4}S)^{3}D	2-3	2p^4-2p^{3}3d	22,23	2,20,27
13.83	208 b	1	Fe XVII	13.824	13.826	^{1}S-^{1}P	0-1	2s^{2}2p^6-2s2p^{6}3p	15,22	16
13.89	40	1	Fe XVII	13.890	13.890	^{1}S-^{3}P	0-1	2s^{2}2p^6-2s2p^{6}3p	15,22	16
13.95	44 b	1	Fe XVIII	13.957	13.955	^{2}P-(^{1}S)^{2}D	3/2-5/2	2p^5-2p^{4}3d	22	1,12
14.03	78 b	1	Fe XIX	14.017	14.039	^{3}P-(^{4}S)^{3}D	1-2	2p^4-2p^{3}3d	22	1,20,27
	b		Ni XIX		14.043	^{1}S-^{3}P	0-1	2p^6-2p^{5}3s	22	14
14.08	48 b	1	Ni XIX	14.076	14.081	^{1}S-^{3}P	0-2	2p^6-2p^{5}3s	22	21
14.11	48 b	1	Fe XVIII	14.124	14.120	^{2}P-(^{1}S)^{2}D	1/2-3/2	2p^5-2p^{4}3d	22,24	1,12
14.15	56 b	1	Fe XVIII	14.152	14.151	^{2}P-(^{1}D)^{2}D	3/2-3/2	2p^5-2p^{4}3d	22,24	1,12
14.20	436 b	1	Fe XVIII	14.204	14.203	^{2}P-(^{1}D)^{2}D	3/2-5/2	2p^5-2p^{4}3d	22	1
14.25	191 b	1	Fe XVIII	14.258	14.255	^{2}P-(^{1}D)^{2}S	3/2-1/2	2p^5-2p^{4}3d	13,22,24	1,12
14.35	107 b	1	Fe XVIII	14.343	14.344	^{2}P-(^{1}D)^{2}P	1/2-1/2	2p^5-2p^{4}3d	22	1
	b		Fe XVIII	14.360	14.361	^{2}P-(^{1}D)^{2}D	1/2-3/2	2p^5-2p^{4}3d		1,12
14.37	184 b	1	Fe XVIII	14.374	14.374	^{2}P-(^{3}P)^{2}D	3/2-5/2	2p^5-2p^{4}3d	13,22	1,12
14.45	86 b	1	Fe XVIII	14.450	14.453	^{2}P-(^{3}P)^{2}D	3/2-3/2	2p^5-2p^{4}3d	22	1
14.53	166 b	1	Fe XVIII	14.536	14.535	^{2}P-(^{3}P)^{2}F	3/2-5/2	2p^5-2p^{4}3d	22	1,12
14.55	62 b	1	Fe XVIII		14.551	^{2}P-(^{3}P)^{2}P	3/2-3/2	2p^5-2p^{4}3d		1
14.67	84	1	Fe XIX	14.666	14.668	^{3}P-^{3}D	2-3	2p^4-2p^{3}3s	22	1,14
14.75	56 b	1	Fe XVIII	14.759	14.766	^{2}P-(^{3}P)^{4}P	1/2-3/2	2p^5-2p^{4}3d	22,24	1,12,18
14.81	56 b	1	O VIII	14.817	14.8206	^{2}S-^{2}P	1/2-1/2 , 3/2	1s-5p	22	6
15.01	1214	1	Fe XVII	15.012	15.013	^{1}S-^{1}P	0-1	2p^6-2p^{5}3d	13,15,22	18
15.18	82 b	1	Fe XIX	15.175	15.172	^{3}P-(^{4}S)^{3}S	1-1	2p^4-2p^{3}3s	22	1,14
	b		O VIII		15.1762	^{2}S-^{2}P	1/2-1/2 , 3/2	1s-4p	22	6
15.21	123	1	Fe XVI?	15.205	15.22			2p^{6}3d-2p^{5}3d^2		22
15.26	700	1	Fe XVII	15.255	15.261	^{1}S-^{3}D	0-1	2p^6-2p^{5}3d	13,15,22	18
15.28	b	1	?	15.289						22
15.38	b	1	?	15.369						22
15.45	138	1	Fe XVII	15.451	15.454	^{1}S-^{3}P	0-1	2p^6-2p^{5}3d	15,22	18
15.49	27	1	Fe XVIII	15.497	15.492	^{2}P-(^{1}S)^{2}S	1/2-1/2	2p^5-2p^{4}3s	22	1,12,18
15.62	185	1	Fe XVIII	15.624	15.625	^{2}P-(^{1}D)^{2}D	3/2-5/2	2p^5-2p^{4}3s	22,24	1,12,18
15.76	53	1	Fe XVIII	15.763	15.765	^{2}P-(^{3}P)^{2}P	3/2-1/2	2p^5-2p^{4}3s	22,24	1,12,18
15.83	150 b	1	Fe XVIII	15.827	15.828	^{2}P-(^{3}P)^{4}P	3/2-3/2	2p^5-2p^{4}3s	22,24	1,12,18
15.87	151	1	Fe XVIII	15.871	15.869	^{2}P-(^{1}D)^{4}D	1/2-3/2	2p^5-2p^{4}3s	22,24	1,12,18
16.00	402 b	1	Fe XVIII	16.003	16.004	^{2}P-(^{3}P)^{2}P	3/2-3/2	2p^5-2p^{4}3s	13,24	1,12
	b		O VIII		16.0059	^{2}S-^{2}P	1/2-1/2 , 3/2	1s-3p	13,22	6
	b		Fe XVIII	16.016	16.025	^{2}P-(^{3}P)^{2}P	1/2-1/2	2p^5-2p^{4}3s	13,22	1,12
16.08	364 b	1	Fe XVIII	16.073	16.072	^{2}P-(^{3}P)^{4}P	3/2-5/2	2p^5-2p^{4}3s	22	1,12,18
16.11	78	1	Fe XVIII	16.107	16.109	^{2}P-(^{3}P)^{4}P	1/2-1/2	2p^5-2p^{4}3s	22	1,12,18
16.17	110 b	1	Fe XVIII	16.165		^{2}S-(^{3}P)^{2}P	1/2-3/2	2p^6-2s2p^{5}3s	22	
16.24	103 b	1	Fe XVIII	16.234		^{2}S-(^{3}P)^{4}P	1/2-1/2	2s2p^6-2s2p^{5}3s		22
16.35	103 b	1	Fe XVIII	16.337		^{2}S-(^{3}P)^{4}P	1/2-5/2	2s2p^6-2s2p^{5}3s		22
16.77	1231	1	Fe XVII	16.775	16.775	^{1}S-^{1}P	0-1	2p^6-2p^{5}3s	13,15,22	18
17.05	1458	1	Fe XVII	17.051	17.051	^{1}S-^{3}P	0-1	2p^6-2p^{5}3s	13,15,22	
17.10	1455	1	Fe XVII	17.069	17.096	^{1}S-^{3}P	0-2	2p^6-2p^{5}3s	13,15,22	
17.62	151	1	Fe	17.622		Uncl			22	
18.36	131	2	Mg XI		9.1685	^{1}S-^{1}P	0-1	1s^2-1s2p		16
18.50	47	1	Cr XV	18.497	18.497	^{1}S-^{1}P	0-1	2p^6-2p^{5}3d	17	
18.63	128	1	O VII	18.626	18.6280	^{1}S-^{1}P	0-1	1s^2-1s3p	13,17,22	7
18.97	1283	1	O VIII	18.970	18.9689	^{2}S-^{2}P	1/2-1/2 , 3/2	1s-2p	13,17,22	6
19.26	34	1	Cr XVI	19.261	19.255	^{2}P-^{2}D	3/2-5/2	2p^5-2p^4(^{1}D)3s	17	
20.86	43	1	Cr XV	20.863	20.863	^{1}S-^{1}P	0-1	2p^6-2p^{5}3s	17	
20.90	29	1	N VII	20.913	20.910	^{2}S-^{2}P	1/2-1/2 , 3/2	1s-3p	17	
21.15	45	1	Cr XV	21.156	21.153	^{1}S-^{3}P	0-1	2p^6-2p^{5}3s	17	
21.20	43	1	Cr XV	21.204	21.208	^{1}S-^{3}P	0-2	2p^6-2p^{5}3s	17	
21.45	37	1	Ca XVI	21.444	21.450	^{2}P-^{2}D	1/2-3/2	2p-3d	17	
21.60	508	1	O VII	21.601	21.6013	^{1}S-^{1}P	0-1	1s^2-1s2p	13,17	
21.80	192	1	O VII	21.807	21.8035	^{1}S-^{3}P	0-1	1s^2-1s2p	13,17	

© American Astronomical Society • Provided by the NASA Astrophysics Data System

1985ApJ...291..865A

TABLE 3—*Continued*

Observed Wavelength A	Intensity	Order	Ion	Previous Solar Wavelength A	Selected Previous Measurement A	Multiplet	J-J'	Transition Array	Solar References	Other References
22.10	398	1	O VII	22.100	22.0975	$^1S-^3S$	0-1	$1s^2-1s2s$	13,17	
22.26	66	2	Fe XVII		11.129	$^1S-^1P$	0-1	$2p^6-2p^5 5d$	15	16
22.50	56	2	Fe XVII		11.250	$^1S-^3D$	0-1	$2p^6-2p^5 5d$		16
22.71	43	1	Ca XV	22.733	22.726	$^3P-^3D$	0-1	$2p^2-2p3d$	17	16
24.09	69 b	1	Ca XIV		24.086	$^4S-^4P$	3/2-3/2	$2p^3-2p^2 3d$		9
24.13	55	1	Ca XIV		24.133	$^4S-^4P$	3/2-5/2	$2p^3-2p^2 3d$		9
24.27	685 b	2	Fe XVII		12.123	$^1S-^1P$	0-1	$2p^6-2p^5 4d$	22	
			Ne X		12.1339	$^2S-^2P$	1/2-1/2, 3/2	1s-2p	22	
24.38	59									
24.53	206	2	Fe XVII		12.263	$^1S-^3D$	0-1	$2p^6-2p^5 4d$	22	
24.63	39	2	Fe XXI		12.285	$^3P-^3D$	0-1	$2p^2-2p3d$	22	2,18
24.68	24	1								
24.78	218	1	N VII		24.781	$^2S-^2P$	1/2-1/2, 3/2	1s-2p		16
24.86	b									
25.98	29	2?	?		12.977				22	
26.03	39	1	Ca XIII		26.033	$^3P-(^2D)^3D$	2-3	$2p^4-2p^3 3d$		9
26.10	28	2	Fe XVIII		13.049	$^2P-(^1P)^2D$	1/2-3/2	$2s^2 2p^5-2s2p^5 3p$	22	1
26.22	23	1	Ca XIII		26.219	$^3P-^3D$	1-2	$2p^4-(^2D)2p^3 3d$		9
26.33	28	2	Fe XVIII		13.159	$^2P-(^3P)^2S$	3/2-1/2	$2s^2 2p^5-2s2p^5 3p$	22	1
26.36	39									
26.48	47	2	Fe XIX		13.288	$^3P-(^2P)^3D$	2-3	$2p^4-2p^3 3d$	23	20,27
26.59	16									
26.64	47									
26.71	28	1	Ca XIII		26.719	$^3P-(^4S)^3D$	2-3	$2p^4-2p^3 3d$		9
26.79	19	2	Fe XVIII		13.374	$^2P-(^3D)^2D$	3/2-5/2	$2s^2 2p^5-2s2p^5 3p$	22	1
26.89	275	2	Ne IX		13.4471	$^1S-^1P$	0-1	$1s^2-1s2p$	22,23	7
26.93	72	2	Fe XIX		13.473	$^3P-^3S$	2-1	$2p^4-2p^3 3d$	22,23	2,14,20,27
27.01	100	2	Fe XIX		13.506(491)	$^3P-(^2P)^3P$	2-2	$2p^4-2p^3 3d$	22,23	2,14,20,27
27.04	100	2	Fe XIX		13.521	$^3P-(^2D)^3D$	2-3	$2p^4-2p^3 3d$	22,23	2,14,20,27
27.10	72	2	Ne IX		13.5529	$^1S-^3P$	0-1	$1s^2-1s2p$	22	7
27.15	39	1								
27.22	27	2			13.630				22	
27.39	251	2	Ne IX		13.6987	$^1S-^3S$	0-1	$1s^2-1s2s$	22	7
27.56	89	2	Ni XIX		13.779	$^1S-^1P$	0-1	$2p^6-2p^5 3s$	22,23	14
27.60		1	Ca XII		27.606	$^2P-^2D$	1/2-3/2	$2p^5-2p^4 3d$		16
		2	Fe XIX		13.796	$^3P-(^4S)^3D$	2-3	$2p^4-2p^3 3d$	23	2,14,20,27
27.65	195	2	Fe XVII		13.826	$^1S-^1P$	0-1	$2s^2 2p^6-2s2p^6 3p$	22,23	16
27.98	61	2	Fe XIX		14.017	$^3P-(^4S)^3D$	1-2	$2p^4-2p^3 3d$	22	27
		1	Ca XII		27.978	$^2P-(^1D)^2P$	3/2-3/2	$2p^5-2p^4 3d$		16
28.08	88	2	Ni XIX		14.043	$^1S-^3P$	0-1	$2p^6-2p^5 3s$	21,22	14
28.13	15 b	2	Ca XII		28.134	$^2P-(^1D)^2P$	3/2-1/2	$2p^5-2p^4 3d$		16
28.15	72	2	Ni XIX		14.081	$^1S-^3P$	0-2	$2p^6-2p^5 3s$	21,22	16
28.25	72	2	Fe XVIII		14.120	$^2P-(^1S)^2D$	1/2-3/2	$2p^5-2p^4 3d$	24	1,12
28.40	546 b	2	Fe XVIII		14.203	$^2P-(^1D)^2D$	3/2-5/2	$2p^5-2p^4 3d$	22	1
28.46	87	1	C VI	28.47	28.466	$^2S-^2P$	1/2-1/2, 3/2	1s-3p	13	16
28.51	126	2	Fe XVIII		14.258	$^2P-(^1D)^2S$	3/2-1/2	$2p^5-2p^4 3d$	24	1,12
28.56		1								16
28.75	162	2	Fe XVIII		14.374	$^2P-(^3P)^2D$	3/2-5/2	$2p^5-2p^4 3d$	22	1,12
28.78	68	1	N VI	28.79	28.787	$^1S-^1P$	0-1	$1s^2-1s2p$	13	
28.91	90	2	Fe XVIII		14.453	$^2P-(^3P)^2D$	3/2-3/2	$2p^5-2p^4 3d$	22	1
29.07	10 #	1	N VI		29.087	$^1S-^3P$	0-1	$1s^2-1s2p$	22	16
		2	Fe XVIII		14.535	$^2P-(^3P)^2F$	3/2-5/2	$2p^5-2p^4 3d$	22	1,12
29.17	b	2	Fe XVIII		14.550	$^2P-(^3P)^4P$	3/2-3/2	$2p^5-2p^4 3d$	22	1,12,18
29.31		2	Fe XIX		14.668	$^3P-^3D$	2-3	$2p^4-2p^3 3s$	22	1,14
29.53	20 #	1	N VI	29.52	29.53	$^1S-^3S$	0-1	$1s^2-1s2s$	13	
		2	Fe XVIII		14.766	$^2P-(^3P)^4P$	1/2-3/2	$2p^5-2p^4 3d$	24	1,12,18
29.65		2	O VIII		14.8206	$^2S-^2P$	1/2-1/2, 3/2	1s-5p	22	6
29.99	29									
30.03	1155	2	Fe XVII	30.02	15.013	$^1S-^1P$	0-1	$2p^6-2p^5 3d$	13,15	18
30.09	b									
30.35	127	2	O VIII		15.1762	$^2S-^2P$	1/2-1/2, 3/2	1s-4p	22	6
			Fe XIX		15.172	$^3P-(^4S)^3S$	1-1	$2p^4-2p^3 3s$	22	1
30.45	134 #	1	Ca XI	30.43	30.445	$^1S-^1P$	0-1	$2p^6-2p^5 3d$	13	16
		1	S XIV	30.428	30.470	$^2S-^2P$	1/2-1/2, 3/2	2s-3p		8
30.52	594 #	2	Fe XVII		15.261	$^1S-^3D$	0-1	$2p^6-2p^5 3d$	15	18
30.56	48	1								
30.60		2			15.289				22	
30.91	105	2	Fe XVII		15.454	$^1S-^3P$	0-1	$2p^6-2p^5 3d$	15	18
31.01	93	1	Si XII		31.015	$^2S-^2P$	1/2-1/2, 3/2	2s-4p		16
		2	Fe XVIII		15.492	$^2P-(^1S)^2S$	1/2-1/2	$2p^5-2p^4 3s$		1,12,18
31.25	174	2	Fe XVIII		15.625	$^2P-(^1D)^2D$	3/2-5/2	$2p^5-2p^4 3s$		1,12,18

© American Astronomical Society • Provided by the NASA Astrophysics Data System

1985ApJ...291..865A

TABLE 3—*Continued*

Observed Wavelength A	Intensity	Order	Ion	Previous Solar Wavelength A	Selected Previous Measurement A	Multiplet	J-J'	Transition Array	Solar References	Other References
31.36	43	2			15.677				22	
31.65	174	2	Fe XVIII		15.828	$^2P-(^3P)^4P$	3/2-3/2	$2p^5-2p^4 3s$		1,12,18
31.74	140	2	Fe XVIII		15.869	$^2P-(^1D)^2D$	1/2-3/2	$2p^5-2p^4 3s$	22	
31.77	22	1								
31.83	14	1								
31.94	22	1	Ca XII		31.960	$^2P-(^1D)^2D$	1/2-3/2	$2p^5-2p^4 3s$		16
32.01	377	2	Fe XVIII		16.004	$^2P-(^3P)^2P$	3/2-3/2	$2p^5-2p^4 3s$	22	
			O VIII		16.0059	$^2S-^2P$	1/2-1/2, 3/2	1s-3p	22	16
32.14	465	2	Fe XVIII		16.072	$^2P-(^3P)^4P$	3/2-5/2	$2p^5-2p^4 3s$	22	
32.19	43	1	S XIII		32.191	$^1S-^3P$	0-1	$2s^2-2s3p$		8
32.24	50	1	S XIII		32.242	$^1S-^1P$	0-1	$2s^2-2s3p$		8
32.29	b	1	Ca XII		32.280	$^2P-^2P$	3/2-3/2	$2p^5-2p^4 3s$		16
32.33	87	2	Fe XVIII		16.165	$^2S-(^3P)^2P$	1/2-3/2	$2s2p^6-2s2p^5 3s$	22	16
32.41	50	1	S XIV		32.407	$^2P-^2D$	1/2-3/2	2p-3d		8
32.47	52	2	Fe XVIII		16.234	$^2S-(^3P)^4P$	1/2-1/2	$2s2p^6-2s2p^5 3s$	22	
32.50	21	1	Ca XII		32.498	$^2P-^4P$	3/2-3/2	$2p^5-2p^4 3s$		16
32.55	95	1	S XIV		32.565	$^2P-^2D$	3/2-5/2	2p-3d		8
32.66	85 b	1	Ca XII		32.655	$^2P-^4P$	3/2-5/2	$2p^5-2p^4 3s$		16
	b		Fe XVI		32.652	$^2P-^2D$	3/2-5/2	3p-7d		16
32.97	28	1	Si XII		32.972	$^2P-^2D$	3/2-5/2	2p-4d		16
33.22	25	2			16.619				22	
33.30	25	1								
33.38	25									
33.50	25	1	Si XI?		33.515	$^1S-^1P$	0-1	$2s^2-2s4p$		16
33.54	1074	2	Fe XVII		16.775	$^1S-^1P$	0-1	$2p^6-2p^5 3s$	15,22	18
33.73	358	1	C VI	33.74	33.7360	$^2S-^2P$	1/2-1/2, 3/2	1s-2p	13	16
33.96	17	1	S XIII		33.951	$^3P-^3D$	2-3	$2s2p-2s3d$		8
34.10	1332	2	Fe XVII		17.051	$^1S-^3P$	0-1	$2p^6-2p^5 3s$	15,22	16
34.19	1447	2	Fe XVII		17.096	$^1S-^3P$	0-2	$2p^6-2p^5 3s$	15,22	16
34.86	22	1	Fe XVI		34.857	$^2P-^2D$	1/2-3/2	3p-6d		16
34.99	33 b	1	C V		34.9728	$^1S-^1P$	0-1	$1s^2-1s3p$		16
35.10	38	1	Fe XVI		35.106	$^2P-^2D$	3/2-5/2	3p-6d		16
35.21	28 b	1	Ca XI	35.22	35.212	$^1S-^1P$	0-1	$2p^6-2p^5 3s$	13	16
35.24	98	2	Fe		17.62	Uncl			22	
35.36	41 b	1	Fe XVI		35.368	$^2D-^2F$	5/2-7/2	3d-8f		16
	b		Si XI		35.35,38	$^3P-^3D$	1-2, 0-1	$2s2p-2s4d$		16
35.46	17	1	Si XI		35.446	$^3P-^3D$	2-3	$2s2p-2s4d$		16
35.57	41	1	Ca XI	35.58	35.576	$^1S-^3P$	0-1	$2p^6-2p^5 3s$	13	16
35.67	97 b	1	S XIII	35.70	35.667	$^1P-^1D$	1-2	$2s2p-2s3d$	13	8
35.73	11	1	Fe XVI		35.71	$^2P-^2S$	1/2-1/2	3p-6s		16
35.80	21	1								
36.01	11	1	Fe XVI		36.01	$^2P-^2S$	3/2-1/2	3p-6s		16
36.12		1								
36.40	48 b	1	S XII	36.39	36.398	$^2P-^2D$	1/2-3/2	$2s^2 2p-2s^2 3d$		8
		3	Ne X		12.1339	$^2S-^2P$	1/2,1/2,3/2	1s-2p	22	16
36.52	33 b									
36.56	34	1	S XII		36.563	$^2P-^2D$	3/2-5/2	$2s^2 2p-2s^2 3d$		16
36.75	48	1	Fe XVI		36.749	$^2S-^2P$	1/2-3/2	3s-5p		16
36.80	49	1	Fe XVI		36.803	$^2S-^2P$	1/2-1/2	3s-5p		16
36.89										
36.93										
37.26	86	2	O VII		18.6280	$^1S-^1P$	0-1	$1s^2-1s3p$	22	16
37.35										
37.42	11	1								
37.60	47	1	S XII		37.603	$^2D-^2F$	5/2-7/2	$2s2p^2-2s2p3d$		8
37.71	13	1	S XII		37.714	$^2D-^2F$	3/2-5/2	$2s2p^2-2s2p3d$		8
37.93	1102	2	O VIII		18.9689	$^2S-^2P$	1/2-1/2,3/2	1s-2p	22	
39.66	35 b	1	Mg X		39.669	$^2S-^2P$	1/2-3/2	2s-5p		16
39.66	35 b	1	Mg X		39.669	$^2S-^2P$	1/2-3/2	2s-5p		16
			S XI		39.648	$^1D-^1F$	2-3	$2s^2 2p^2-2s^2 2p3d$		8
39.75	16									
39.83	78	1	Fe XVI		39.827	$^2P-^2D$	1/2-3/2	3p-5d		16
39.89										
39.94										
40.14	122	1	Fe XVI		40.153	$^2P-^2D$	3/2-5/2	2p-5d		16
40.19	32	1	Fe XVI		40.199	$^2D-^2F$	3/2-5/2	3d-6f		16
40.27	132 b	1	C V	40.27	40.2680	$^1S-^1P$	0-1	$1s^2-1s2p$	13	16
			(Fe XVI		40.245	$^2D-^2F$	5/2-7/2	3d-6f)		16
40.34		3	Ne IX		13.4471				22	
40.53		3	Fe XIX		13.506				22	
40.56		3	Fe XIX		13.521				22	
40.66		3	Ne IX		13.551				22	

© American Astronomical Society • Provided by the NASA Astrophysics Data System

1985ApJ...291..865A

TABLE 3—*Continued*

Observed Wavelength A	Intensity	Order	Ion	Previous Solar Wavelength A	Selected Previous Measurement A	Multiplet	J-J'	Transition Array	Solar References	Other References
40.72	77	1	C V	40.73	40.7306	$^1S-^3P$	0-1	$1s^2-1s2p$	13	16
40.86	17									
40.91	110	1	Si XII	40.91	40.911	$^2S-^2P$	1/2-3/2	2s-3p	13	16
40.95	58	1	Si XII		40.951	$^2S-^2P$	1/2-1/2	2s-3p		16
41.01	21 b	1	Ni XVIII		41.015	$^2S-^2P$	1/2-3/2	3s-4p		16
41.09	b	3	Ne IX		13.6987				22	
41.22	16 b	1	Ni XVIII		41.218	$^2S-^2P$	1/2-1/2	3s-4p		16
			Fe XIX		13.738					
41.47	16#b	1	C V	41.47		$^1S-^3S$	0-1	$1s^2-1s2s$	13	16
		3	Fe XVII		13.826				22	16
41.90	31	1	Fe XVI		41.91	$^2P-^2S$	1/2-1/2	3p-5s		16
			Fe XV		41.903	$^3P-^3D$	2-3	3s3p-3s5d		16
42.27	31	1	Fe XVI		42.30	$^2P-^2S$	3/2-1/2	3p-5s		16
42.56	27	1	S X	42.53	42.543	$^4S-^4P$	3/2-5/2	$2p^3-2p^23d$	13	8
42.61		3	Fe XVIII		14.204				22	
43.20	385	2	O VII		21.6013	$^1S-^1P$	0-1	$1s^2-1s2p$		16
43.29	32 b	1	Si XI	43.22	43.290	$^3P-^3D$	2-3	2s2p-2p3p	13	16
43.61	176	2	O VII	43.66	21.8035	$^1S-^3P$	0-1	$1s^2-1s2p$	13	16
43.65	21	1								
43.75	90	1	Si XI	43.74	43.763	$^1S-^1P$	0-1	$2s^2-2s3p$	13	16
43.80	21 b	1	Ni XVIII		43.814	$^2P-^2D$	1/2-3/2	3p-4d		16
44.02	138 b	1	Si XII	44.02	44.021	$^2P-^2D$	1/2-3/2	2p-3d	13	16
			(Mg X		44.050	$^2S-^2P$	1/2-3/2	2s-4p)		16
44.16	224 b	1	Si XII	44.17	44.165	$^2P-^2D$	3/2-5/2	2p-3d	13	16
44.20	292	2	O VII		22.0975	$^1S-^3S$	0-1	1s2s-1s3s	13	
44.36	32	1	Ni XVIII		44.365	$^2P-^2D$	3/2-5/2	2p-3d		16
45.04		3	Fe XVII		15.013				22	
45.51	57	1	Si XII	45.52	45.519	$^2P-^2S$	1/2-1/2	2p-3s	13	16
45.68	109	1	Si XII	45.68	45.692	$^2P-^2S$	3/2-1/2	2p-3s	13	16
45.73										
45.76										
45.79		3	Fe XVII		15.261				22	
46.18		1								
46.30	55	1	Si XI		46.300	$^3P-^3D$	1-2	2s2p-2s3d		16
46.40	50	1	Si XI	46.41	46.401	$^3P-^3D$	2-3	2s2p-2s3d	13	16
46.66	60	1	Fe XVI		46.661	$^2D-^2F$	3/2-5/2	3d-5f		16
46.72	83	1	Fe XVI		46.718	$^2D-^2F$	5/2-7/2	3d-5f		16
47.32	23	1	Mg X		47.310	$^2P-^2D$	3/2-5/2	2p-4d		16
47.67	38 b	1	Ni XVII		47.663	$^1P-^1D$	1-2	2s3p-2s4d		16
	b		(Si XI?		47.653	$^3P-^3D$	2-3	$2p^2-2p3d$)		16
47.79	30		Ni XVI		47.772	$^2P-^2D$	3/2-5/2	3d-4d		16
48.02		3	Fe XVIII		16.004				22	
			O VIII		16.0059				22	
48.22		3	Fe XVIII		16.072				22	
48.25	b									
48.29	20 b	1	Aℓ XI		48.297	$^2S-^2P$	1/2-3/2	2s-3p		16
48.33	25 b	1	Aℓ XI		48.338	$^2S-^2P$	1/2-1/2	2s-3p		16
			Mg IX		48.340	$^1S-^1P$	0-1	$2s^2-2s4p$		16
48.97	22	1	Fe XVI		48.97	$^2D-^2P$	5/2-3/2	3d-5p		16
49.18		1	Si XI		49.181	$^3P-^3S$	2-1	2s2p-2s3s		16
49.22	118	1	Si XI	49.22	49.222	$^1P-^1D$	1-2	2s2p-2s3d	13	16
49.31	b	1								
49.49		1	Fe XV		49.49	$^1D-^1F$	2-3	3s3d-3s4f		16
49.56	207	2	N VII		24.781	$^2S-^2P$	1/2-1/2, 3/2	1s-2p		16
49.64										
49.71	43									
49.76	22	2	N VI		24.898	$^1S-^1P$	0-1	$1s^2-1s3p$		16
49.81										
49.88	12									
50.01	30 b									
50.26	39	1	Ni XVIII		50.27	$^2P-^2S$	1/2-1/2	3p-4s		16
50.32		3	Fe XVII		16.775				22	
50.35	195	1	Fe XVI	50.36	50.350	$^2S-^2P$	1/2-3/2	3s-4p	13	16
50.52	12 b	1	Si X	50.53	50.524	$^2P-^2D$	1/2-3/2	$2s^22p-2s^23d$	13	16
50.56	98	1	Fe XVI		50.555	$^2S-^2P$	1/2-1/2	3s-4p		16
50.63	12									
50.69	74	1	Si X	50.69	50.691	$^2P-^2D$	3/2-5/2	$2s^22p-2s^23d$	13	16
51.02	22	1	Ni XVIII		51.02	$^2P-^2S$	3/2-1/2	3p-4s		16
51.15		3	Fe XVII		17.051				22	
51.28		3	Fe XVII		17.096				22	
51.96	10		Aℓ X		51.979	$^1S-^3P$	0-1	$2s^2-2s3p$		26
52.05										
52.09	10								22	16

© American Astronomical Society • Provided by the NASA Astrophysics Data System

1985ApJ...291..865A

TABLE 3—*Continued*

Observed Wavelength A	Intensity	Order	Ion	Previous Solar Wavelength A	Selected Previous Measurement A	Multiplet	J-J'	Transition Array	Solar References	Other References
52.26	12									16
52.30	88	1	Si XI	52.30	52.296	^1P-^1S	1-0	2s2p-2s3s	13	16
			Aℓ XI		52.244	^2P-^2D	1/2-3/2	2p-3d	16	
52.36										
52.42	18#b	1	Aℓ XI		52.446	^2P-^2D	3/2-5/2	2p-3d		16
52.48	15									
52.61	40	1	Ni XVIII		52.615	^2D-^2F	3/2-5/2	3d-4f		16
52.72	31	1	Ni XVIII		52.720	^2D-^2F	5/2-7/2	3d-4f		16
52.91	66	1	Fe XV		52.911	^1S-^1P	0-1	$3s^2$-3s4p		16
53.11	31 b	1								
54.13	157	1	Fe XVI	54.15	54.142	^2P-^2D	1/2-3/2	3p-4d	13,19	16
54.36	16 b									
54.40	14 b	1	Aℓ XI		54.399	^2P-^2S	3/2-1/2	2p-3s		16
54.45	16 b									
54.57										
54.60	12									
54.72	223	1	Fe XVI	54.70	54.728	^2P-^2D	3/2-5/2	3p-4d	13	16
54.77	36	1	Fe XVI		54.769	^2P-^2D	3/2-3/2	3p-4d	19	16
54.90										
55.11	17	1	Si X	55.06	55.096	^2P-^2S	3/2-1/2	$2s^2 2p$-$2s^2 3s$	13	16
55.16	17	1	Ni XVII		55.173	^3D-^3F	2-3	2s3d-2s4f		16
55.23		1	Si IX		55.234	^3P-^3P	2-1	$2p^2$-2p3d		16
55.28	28	1	Ni XVII	55.30	55.248	^3D-^3F	3-4	2s3d-2s4f	13,19	16
			Si IX		55.272	^3P-^3P	2-2	$2p^2$-2p3d		16
			Aℓ X		55.272	^3P-^3D	1-2	2s2p-2s3d		16
55.37	22	1	Si IX		55.356	^3P-^3D	1-2	$2p^2$-2p3d		16
			Aℓ X		55.376	^3P-^3D	2-3	2s2p-2s3d		16
55.41	43	1	Si IX		55.401	^3P-^3D	2-3	$2p^2$-2p3d		16
55.50										
55.55										
55.78	28		Fe XV		55.793	^3P-^3D	1-2	3s3p-3s4d		16
55.97	14									16
56.04	20	1	Si IX		56.027	^1D-^1F	2-3	$2p^2$-2p3d		16
56.17	46	1	Fe XV	56.12	56.200	^3P-^3D	2-3	3s3p-3s4d	13	16
56.21										
56.30	14 b									
56.91		3	O VIII	56.92	18.97				13	16
56.95	80 b	2	C VI		28.466	^2S-^2P	1/2-1/2, 3/3	1s-3p		16
57.14	2	2			28.56					
			Si X?		57.209	^2D-^2P	5/2-3/2	$2s2p^2$-$2s2p3s$		16
57.20	25									
			Si X?		57.365	^2D-^2P	3/2-1/2	$2s2p^2$-$2s2p3s$		
57.35	17 b									
57.43										
57.48										
57.57	20#b	2	N VI	57.56	28.787	^1S-^1P	0-1	$1s^2$-1s2p	13	16
57.71	11	4	Fe XVIII		14.418				22	
57.88	107	1	Mg X	57.88	57.876	^2S-^2P	1/2-3/2	2s-3p	13,19	16
57.92	54	1	Mg X		57.920	^2S-^2P	1/2-1/2	2s-3p		16
58.79	11		Aℓ X		58.808	^3P-^3S	0-1	2s2p-2s3s		16
58.92	17 b		Si VIII		58.885	^4S-^4P	3/2-5/2	$2s^2 2p^3$-$2s2p^3 3p$		16
58.96	29 b	1	Fe XIV	58.97	58.963	^2P-^2D	1/2-3/2	3p-4d	13,19	16
59.08		2	N VI		29.53	^1S-^3S	0-1	$1s^2$-1s2s	13	16
59.40	85	1	Fe XV	59.42	59.404	^1P-^1D	1-2	3s3p-3s4d	13	16
59.59	42#b	1	Fe XIV	59.62	59.579	^2P-^2D	3/2-5/2	3p-4d	13	16
60.81	11		Mg VIII		60.806	^2P-^2S	3/2-1/2	2p-4s		16
60.89	b		Aℓ IX		60.896	^2P-^2D	1/2-3/2	2p-3d	5,13	16
61.03	17 b	1	Si VIII	61.009	60.989	^4S-^4P	3/2-1/2	$2p^3$-$2p^2 3d$		16
					61.019	^4S-^4P	3/2-3/2	$2p^3$-$2p^2 3d$	5	16
61.09	24 b	1	Si VIII	61.081	61.070	^4S-^4P	3/2-5/2	$2p^3$-$2p^2 3d$	5,13,19	16
			Aℓ IX		61.069	^2P-^2D	3/2-5/2	2p-3d		16
			Mg IX?		61.088,127	^3P-^3P	1-1, 2-2	2s2p-2p3p		16
61.19		1	Si VIII		61.175	^4S-^4D	3/2-1/2	$2p^3$-$2p^2 3d$		16
			Mg IX?		61.175	^3P-^3P	2-1	2s2p-2p3p		16
61.23			Si VIII		61.223	^4S-^4D	3/2-5/2	$2p^3$-$2p^2 3d$		16
61.61	18	1	Si IX		61.600	^3P-^3P	0-1	$2p^2$-2p3s		16
61.66		1	Si IX	61.66	61.649	^3P-^3P	2-2	$2p^2$-2p3s		16
61.85	21	1	Si IX	61.841	61.852	^3P-^3P	2-1	$2p^2$-2p3s	13	16
			Si VIII		61.852	^2D-$(^1D)^2D$	5/2-5/2	$2p^3$-$2p^2 3d$	5	16
61.92	32	1	Si VIII	61.912	61.914	^2D-$(^1D)^2F$	5/2-7/2	$2p^3$-$2p^2 3d$	5,13	16
			Mg IX		61.924	^3P-^3D	2-3	2s2p-2p3p		16
62.36		1	Fe XIII?	62.35	62.354			$2p^2$-2p4d	13	11
62.68	11	1	Fe XIII		62.694	^3P-^3D	1-2	$2p^2$-2p4d		11

© American Astronomical Society • Provided by the NASA Astrophysics Data System

1985ApJ...291..865A

TABLE 3—*Continued*

Observed Wavelength A	Intensity	Order	Ion	Previous Solar Wavelength A	Selected Previous Measurement A	Multiplet	J-J'	Transition Array	Solar References	Other References
62.75	39	1	Mg IX	62.755	62.751	$^1S-^1P$		$2s^2-2s3p$	5,13,19	16
62.88	196	1	Fe XVI	62.876	62.879	$^2P-^2S$	1/2-1/2	3p-4s	5,13,19	16
62.98	21 b	1	Fe XIII	63.048	62.975	$^3P-^3D$	2-3	$2p^2-2p4d$	5	11
63.16	93	1	Mg X	63.153	63.152	$^2P-^2D$	1/2-3/2	2p-3d	5,13,19	16
63.30	171	1	Mg X	63.294	63.295	$^2P-^2D$	3/2-5/2	2p-3d	5,13,19	16
63.57										
63.72	352	1	Fe XVI	63.714		$^2p-^2S$	3/2-1/2	3p-4s	5,13,19	16
63.97	21	1								
			Aℓ VIII		63.965	$^3p-^3D$	1-2	$2s^22p^2-2s2p^23p$		16
			Aℓ VIII		64.004	$^3p-^3D$	2-3	$2s^22p^2-2s2p^23p$		16
64.12	14 b									
64.16	14 b									
64.34										
65.60	10	1	Mg IX		65.609	$^1P-^1D$	1-2	2s2p-2p3p	19	16
65.66	49	1	Mg X		65.672	$^2P-^2S$	1/2-1/2	2p-3s		16
65.84	97	1	Mg X	65.84	65.847	$^2P-^2S$	3/2-1/2	2p-3s	5,13,19	16
65.90	17									
66.25	221	1	Fe XVI	66.251	66.263	$^2D-^2F$	3/2-5/2	3d-4f	5,19	16
66.36	280	1	Fe XVI	66.356	66.368	$^2D-^2F$	5/2-7/2	3d-4f	5,19	16
67.12		4	Fe XVII		16.775					
	11 b		Mg IX		67.090	$^3P-^3D$	0-1	2s2p-2s3d		16
67.15	17 b	1	Mg IX	67.132	67.135	$^3P-^3D$	1-2	2s2p-2s3d	5	16
67.24	42 b	1	Mg IX	67.223	67.239	$^3P-^3D$	2-3	2s2p-2s3d	5	16
67.38	41	1	Ne VIII		67.382	$^2S-^2P$	1/2-1/2, 3/2	2s-4p		16
67.47		2	C VI		33.7360	$^2S-^2P$	1/2-1/2, 3/2	1s-2p		16
67.61	10	1								
67.69	10	1								
68.22		4	Fe XVII		17.051				22	16
68.37		4	Fe XVII		17.096				22	16
68.51	14	1								
68.85	10	1	Si VIII		68.853	$^4S-^4P$	3/2-3/2	$2p^3-2p^23s$		16
69.65	256	1	(Si VIII	69.658	69.632	$^4S-^4P$	3/2-5/2	$2p^3-2p^23s$	5,13	16
		and	Fe XIV Minor		69.66	$^2P-^2S$	1/2-1/2	3p-4s		16
			Components with some unidentified line contributing main intensity)							
69.71										
69.84	14 b	1	Si VIII		69.790	$^4S-^4P$	3/2-3/2	$2p^3-2p^23s$		
69.89	14 b	1	Si VIII		69.905	$^4S-^4P$	3/2-1/2	$2p^3-2p^23s$		16
69.93	24 b	1	Fe XV	69.939	69.945	$^3D-^3F$	1-2	3s3d-3s4f	5,13	16
69.98	28 b	1	Fe XV		69.987	$^3D-^3F$	2-3	3s3d-3s4f		16
70.05	62	1	Fe XV	70.051	70.054	$^3D-^3F$	3-4	3s3d-3s4f	5,13,19	16
70.60	17	1	Fe XIV		70.613	$^2P-^2S$	3/2-1/2	3p-4s		16
71.00	33	1								
71.11	15									
71.34	44									
71.46										
71.91	48	1	Mg IX	71.919	71.901	$^3P-^3S$	1-1	2s2p-2s3s	5,13	16
72.02	41#b	1	Mg IX	72.030	72.027	$^3P-^3S$	2-1	2s2p-2s3s	5	16
72.30	66	1	Mg IX	72.311	72.312	$^1P-^1D$	2-3	2s2p-2p3d	5,13	16
		1	Si VIII		72.324	$^2P-^2D$	3/2-5/2	$2p^3-2p^23s$		16
72.41	19	1	Si VIII		72.420	$^2D-^2P$	1/2-1/2	$2p^3-2p^23s$		16
73.25	10	1								
73.31	10 b	1								
73.36	10 b	1								
73.39		1								
73.47	123	1	Fe XV	73.471	73.473	$^1D-^1F$	2-3	3s3d-3s4f	5,13,19	11
74.32	20 b	1								
74.36	27 b									
74.40	14 b	1								
74.63		1	Ne VIII		74.637	$^2P-^2S$	3/2-1/2	2p-4s		16
74.86	46	1	Mg VIII	74.854	74.858	$^2P-^2D$	1/2-3/2	2p-3d	5,13,19	16
75.03	88	1	Mg VIII	75.034	75.034	$^2P-^2D$	3/2-5/2	2p-3d	5,13,19	16
75.36		1	Aℓ VII		75.360	$^4S-^4P$	3/2-5/2	$2p^3-2p^2(^3P)3d$		16
75.59										
75.87		4	O VIII	75.887	18.9689					16
		1	Fe XIII		75.892	$^3p-^3p$	2-1	$3p^2-3p4s$	5	11
76.03	55	1	Fe XIV	76.023	76.022	$^2D-^2F$	3/2-5/2	3d-4f		11
76.12	52#	1	Fe XIII		76.117	$^1D-^1P$		$3p^2-3p4s$	5	11
76.16	21#	1	Fe XIV		76.152	$^2D-^2F$	5/2-7/2	3d-4f		11
76.44		1								
76.50	81	1	Fe XVI	76.507	76.502	$^2D-^2P$	5/2-3/2	3d-4p	5	11
76.80	33	1	Fe XVI		76.796	$^2D-^2P$	3/2-1/2	3d-4p		11
77.73	54 b	1	Mg IX	77.741	77.737	$^1P-^1S$	1-0	2s2p-2s3s	5	16
			Na IX		77.764	$^2P-^2D$	1/2-3/2	2p-3d		16

© American Astronomical Society • Provided by the NASA Astrophysics Data System

1985ApJ...291..865A

TABLE 3—*Continued*

Observed Wavelength Å	Intensity	Order	Ion	Previous Solar Wavelength Å	Selected Previous Measurement Å	Multiplet	J-J'	Transition Array	Solar References	Other References
77.88	11#									
78.46a	16									
81.14	17									
82.76	64 b									
88.10	106	1	Ne VIII	88.10	88.092	^2S-^2p	1/2-3/2	2s-3p		16
89.76	63 b									
91.01	42									
93.53	23									
93.84	581		Fe XVIII		93.94	^2p-^2S	3/2-1/2	$2s^22p^5$-$2s2p^6$		16

[a] Wavelengths beyond 77.88 Å are not well determined.
[b] Blend.
[#] Intensity corrected for blend.
* Units = photons cm^{-2} s^{-1} $arcsec^{-2}$.

REFERENCES: (1) Bromage *et al.* 1977. (2) Bromage and Fawcett 1977*a*. (3) Bromage and Fawcett 1977*b*. (4) Bromage, Fawcett, and Cowan 1977. (5) Behring *et al.* 1972. (6) Erickson 1977. (7) Ermolaev and Jones 1974. (8) Fawcett and Hayes 1973. (9) Fawcett and Hayes 1975. (10) Fawcett, Cowan, and Hayes 1972. (11) Fawcett *et al.* 1972. (12) Feldman *et al.* 1973. (13) Freeman and Jones 1970. (14) Gordon *et al.* 1980. (15) Hutcheon *et al.* 1976. (16) Kelly and Palumbo 1973. (17) McKenzie and Landecker 1982*a*. (18) McKenzie *et al.* 1980. (19) Malinovsky and Heroux 1973. (20) Mason *et al.* 1979. (21) Parkinson 1975. (22) Phillips *et al.* 1982. (23) Pye *et al.* 1977. (24) Rugge and Walker 1978. (25) Kastner *et al.* 1974. (26) Fawcett 1984*a*. (27) Fawcett 1984*b*. Reference 22 usually also applies to Reference 18.

sented here reveal new spectral identifications made possible partly because of increased resolving power. Several density-sensitive lines are found in this interval, and modest spectrograph improvements will permit study of X-ray line widths and profiles. Further observations under a variety of solar conditions and extending to longer wavelengths will certainly add much to the knowledge of the solar spectrum.

This work is the culmination of a long collaboration with G. Schmidtke of Institut für Physikalische Messtechnik, Freiburg, the inventor of the diffraction-filter spectrograph slit. We acknowledge useful discussions with A. Franks and his colleagues of the National Physical Laboratory and their contributions to the manufacture of the spectrograph optics. R. Caravalho and S. Salat deserve our thanks for their skillful work on the instrument.

Bob Swindell of Amersham Corporation was helpful in arranging for the autoradiography experiments which were carried out at Amersham International in the UK. We are grateful to Ted Tarbell for assistance in the use of the PDS microdensitometer.

We acknowledge with appreciation the financial support of the NASA Solar Physics office and the excellent rocket and range support by personnel of Goddard Space Flight Center, White Sands Missile Range, and the Lockheed SPARCS team. Richard Hoover of Marshall Space Flight Center generously loaned an X-ray mirror for our laboratory calibration facility. R. Bonnet and M. Decaudin of Laboratoire de Physique Stellaire et Planétaire have contributed much to the success of this experiment in planning and in the field.

The careful work of the referee and the editorial staff at the *Astrophysical Journal* is gratefully acknowledged.

This work has been supported by NASA through contracts NAS 2-6723, NAS 5-25727, and NAS 5-23758, as well as by the Lockheed Independent Research program. The Freiburg contribution was supported by the FRG Bundesministerium für Bildung und Wissenschaft.

REFERENCES

Acton, L. W., Brown, W. A., Bruner, M. E. C., Haisch, B. M., and Strong, K. T. 1983, *Solar Phys.*, **86**, 79.
Askins, B. S., Craven, P. D., and O'Dell, C. R. 1979, *Pub. A.S.P.*, **91**, 724.
Askins, B. S., and O'Dell, C. R. 1980, *Pub. A.S.P.*, **92**, 375.
Bearden, J. A. 1967, *Rev. Mod. Phys.*, **39**, 78.
Behring, W. E., Cohen, L., and Feldman, U. 1972, *Ap. J.*, **175**, 493.
Bonnet, R. M., Bruner, E. C., Acton, L. W., Brown, W. A., and Decaudin, M. 1980, *Ap. J. (Letters)*, **237**, L47.
Bromage, G. E., Cowan, R. C., Fawcett, B. C., Gordon, H., Hobby, M. G., Peacock, N. J., and Ridgeley, A. 1977, *Culham Lab. Rept.* No. CLM-R170 (London: HMSO).
Bromage, G. E. and Fawcett, B. C. 1977*a*, *M.N.R.A.S.*, **178**, 591 and 605.
———. 1977*b*, *M.N.R.A.S.*, **179**, 683.
Bromage, G. E., Fawcett, B. C., and Cowan, R. D. 1977, *M.N.R.A.S.*, **178**, 599.
Brown, W. A., Bruner, E. C., Jr., Acton, L. W., Franks, A., Stedman, M., and Speer, R. J. 1979, *Proc. SPIE*, **184**, 278.
Bruner, E. C., Jr., Brown, W. A., Salat, S. W., Franks, A., Schmidtke, G., Schweizer, W., and Speer, R. J. 1980, *Opt. Eng.*, **19**, 433.
Cohen, L., and Feldman, U. 1970, *Ap. J. (Letters)*, **160**, L105.
Erickson, G. W. 1977, *J. Phys. Chem. Ref. Data*, **6**, 831.
Ermolaev, A. M., and Jones, M. 1974, *J. Phys. B*, **7**, 199.
Ershov, O. A., Brytov, I. A., and Lukirskii, A. P. 1967, *Optics and Spectros.*, **22**, 66.
Fawcett, B. C. 1984*a*, *Atomic Data Nuclear Data Tables*, **30**, 26.
Fawcett, B. C. 1984*b*, private communication.
Fawcett, B. C., Cowan, R. D., and Hayes, R. W. 1972, *J. Phys. B*, **5**, 2143.
Fawcett, B. C., Cowan, R. D., Kononov, E. Y., and Hayes, R. W. 1972. *J. Phys. B*, **5**, 1255.
Fawcett, B. C. and Hayes, R. W. 1973, *Phys. Scripta*, **8**, 244.
———. 1975, *M.N.R.A.S.*, **170**, 185.
Feldman, U., Doschek, G. A., Cowan, R. D., and Cohen, L. 1973, *J. Opt. Soc. Am.*, **63**, 1445.
Freeman, F. F., and Jones, B. B. 1970, *Solar Phys.*, **15**, 288.
Gordon, H., Hobby, M. G., and Peacock, N. J. 1980, *Culham Lab. Rept.*, No. CLM-P592 (London: HMSO).
Hutcheon, R. F., Pye, J. P., and Evans, K. D. 1976, *Astr. Ap.*, **51**, 451.
Kastner, S. O., Neupert, W. M., and Swartz, M. 1974, *Ap. J.*, **191**, 261.
Kelly, R. L., and Palumbo, L. J. 1973, NRL Rept. No. 7599. (Washington: US Govt. Printing Office).
Malinovsky, M., and Heroux, L. 1973, *Ap. J.*, **181**, 1009.
Manson, J. E. 1972, *Solar Phys.*, **27**, 107.
Mason, H. E., Doschek, G. A., Feldman, U., and Bhatia, A. K. 1979, *Astr. Ap.*, **73**, 74.
McKenzie, D. L., and Landecker, P. B. 1982*a*, *Ap. J.*, **254**, 309.
———. 1982*b*, *Ap. J.*, **259**, 372.
McKenzie, D. L., Landecker, P. B., Broussard, R. M., Rugge, H. R., Young, R. M., Feldman, U., and Doschek, G. A. 1980, *Ap. J.*, **241**, 409.
Parkinson, J. H. 1975, *Solar Phys.*, **42**, 183.

© American Astronomical Society • Provided by the NASA Astrophysics Data System

1985ApJ...291..865A

Parmar, A. N., Wolfson, C. J., Culhane, J. L., Phillips, K. J. H., Acton, L. W., Dennis, B. R., and Rapley, C. G. 1984, *Ap. J.*, **279**, 866.
Phillips, K. J. H., *et al.* 1982, *Ap. J.*, **256**, 774.
Pye, J. P., Evans, K. D., and Hutcheon, R. J. 1977, *M.N.R.A.S.*, **178**, 611.
Rugge, H. R., and Walker, A. B. C., Jr. 1978, *Ap. J.*, **219**, 1068.
Schmidtke, G. 1970, *Appl. Optics*, **9**, 447.
Schweizer, W., and Schmidtke, G. 1971, *Ap. J. (Letters)*, **169**, L27.
Widing, K. G., and Sandlin, G. D. 1968, *Ap. J.*, **152**, 545.

LOREN W. ACTON, MARILYN E. BRUNER, and WILLAIM A. BROWN: Lockheed Research Laboratory, Dept. 91-20, Bldg. 255, 3251 Hanover St., Palo Alto, CA 94304

BRIAN C. FAWCETT: Rutherford & Appleton Laboratories, Chilton, Didcot, Oxfordshire 0X11 0QX, England

WERNER SCHWEIZER: Fraunhofer Institut fur Physikalische Messtechnik, Heidenhofstrasse 8, Freiburg i.Br., D7800 West Germany

ROBERT J. SPEER: Blackett Laboratory, Imperial College of Science and Technology, London SW7 2BZ, England

© American Astronomical Society • Provided by the NASA Astrophysics Data System